

Parvaneh, Mohammad Hasan; Khorasani, Pouria Goharshenasan

## Article

# A new hybrid method based on fuzzy logic for maximum power point tracking of photovoltaic systems

Energy Reports

## Provided in Cooperation with:

Elsevier

*Suggested Citation:* Parvaneh, Mohammad Hasan; Khorasani, Pouria Goharshenasan (2020) : A new hybrid method based on fuzzy logic for maximum power point tracking of photovoltaic systems, Energy Reports, ISSN 2352-4847, Elsevier, Amsterdam, Vol. 6, pp. 1619-1632, <https://doi.org/10.1016/j.egy.2020.06.010>

This Version is available at:

<https://hdl.handle.net/10419/244150>

### Standard-Nutzungsbedingungen:

Die Dokumente auf EconStor dürfen zu eigenen wissenschaftlichen Zwecken und zum Privatgebrauch gespeichert und kopiert werden.

Sie dürfen die Dokumente nicht für öffentliche oder kommerzielle Zwecke vervielfältigen, öffentlich ausstellen, öffentlich zugänglich machen, vertreiben oder anderweitig nutzen.

Sofern die Verfasser die Dokumente unter Open-Content-Lizenzen (insbesondere CC-Lizenzen) zur Verfügung gestellt haben sollten, gelten abweichend von diesen Nutzungsbedingungen die in der dort genannten Lizenz gewährten Nutzungsrechte.

### Terms of use:

*Documents in EconStor may be saved and copied for your personal and scholarly purposes.*

*You are not to copy documents for public or commercial purposes, to exhibit the documents publicly, to make them publicly available on the internet, or to distribute or otherwise use the documents in public.*

*If the documents have been made available under an Open Content Licence (especially Creative Commons Licences), you may exercise further usage rights as specified in the indicated licence.*



<https://creativecommons.org/licenses/by/4.0/>



## Research paper

# A new hybrid method based on Fuzzy Logic for maximum power point tracking of Photovoltaic Systems



Mohammad Hasan Parvaneh<sup>a,b,\*</sup>, Pouria Goharshenasan Khorasani<sup>a</sup>

<sup>a</sup> West Regional Electrical Company, Kermanshah, Iran

<sup>b</sup> Department of Electrical Engineering, Faculty of Engineering, Bu Ali Sina University, Hamadan, Iran

## ARTICLE INFO

## Article history:

Received 2 December 2019

Received in revised form 3 June 2020

Accepted 15 June 2020

Available online xxxxx

## Keywords:

Maximum power point tracking (MPPT)

Photovoltaic system

Short Circuit Current (SCC)

Fuzzy Logic (FL)

## ABSTRACT

Solar panels have non-linear voltage–current features with only one distinctive point where maximum power is obtained. This optimal power point alters with oscillations in temperature and radiation intensity. Various techniques have been proposed for online, offline and hybrid maximum power point tracking of photovoltaic systems has been proposed. At first, this algorithm presents a comparison of two components, including work point calculation and accurate adjustment. Then, work point calculation estimates the maximum power point. Finally, accurate adjustment follows the accurate value of maximum power based on Fuzzy Logic (FL) method. The method proposed in this study is simulated in MATLAB/SIMULINK work space. The proposed method is able to improve the dynamic response and steady-state response of the PV systems and a comparison is made between the results of simulation and the existing techniques and the efficacy of the proposed method has been discussed.

© 2020 The Authors. Published by Elsevier Ltd. This is an open access article under the CC BY-NC-ND license (<http://creativecommons.org/licenses/by-nc-nd/4.0/>).

## 1. Introduction

Energy crisis and environmental factors like pollution, global warming and the greenhouse effect are provocative elements that draw the attention of governments to renewable energy resources for replacing conventional fossil-fueled electricity generation. Among available renewable energy generation technologies, solar photovoltaic (PV) arrays have been widely adopted because solar energy is readily available, clean, and PV technologies are low maintenance (Tey et al., 2018; Seyedmahmoudian et al., 2019b; Radjai et al., 2014; Safari and Mekhilef, 2011; Seyedmahmoudian et al., 2015). So, Photovoltaic (PV) system has received much attention from among these sources. The PV system must be controlled in different conditions to work on its maximum power point and the output characteristics of PV solar panel rely on many operating conditions such as irradiance, temperature, Spectral of sunlight, dirt, and shadows. Therefore, an adaptable converter and selection of an impressive and valid (maximum power point tracking, MPPT) algorithm are required to accede and transfer the maximum power from the PV panel to the load under any changes of weather conditions (Radjai et al., 2015). Several issues like the low energy conversion efficiency and heavy dependence on environmental factors, including solar

irradiance and ambient temperature of PV systems remain a serious preventive to utilization of PV power generation and achieving the accurate maximum power point tracking (MPPT) is vitally important (Seyedmahmoudian et al., 2016, 2019a).

This maximum power point, which relies on the load conditions, cell temperature (T) and solar radiation (G), is tracked by MPPT (Koofigar, 2016). The duty-cycle (D) computed by MPPT controller is given to PWM pulse, which is used to adjust the produced band width by PWM. Then, the pulse with controlled width is given to boost the convertor to track the maximum power point. To decrease the costs of PV systems, a critical issue in designing optimal systems is extracting maximum power from a solar panel. In this literature, various methods have been introduced for maximum power point tracking (MPPT). These techniques are differentiated based on different features, such as different kinds of the required sensors, convergence velocity, value, effectiveness range, requirements of hardware implementation and popularity (Tey and Mekhilef, 2015). However, MPPT methods can be classified into online, offline and hybrid types. These techniques are also categorized as Open Circuit Voltage (OCV), Short Circuit Current (SCC) and Artificial Intelligence (AI) methods. Online techniques, also called model-free methods, typically use temporal voltage value or PV output current to produce control signal. Online methods include IC, ESC and P&O (Tey and Mekhilef, 2015). Hybrid methods are also a blend of online and offline methods. In Jain and Agarwal (2007) and Kim (2007), MPPT was presented for PV systems by sliding mode controller

\* Corresponding author at: West Regional Electrical Company, Kermanshah, Iran.

E-mail address: [mhpelectronicman@gmail.com](mailto:mhpelectronicman@gmail.com) (M.H. Parvaneh).

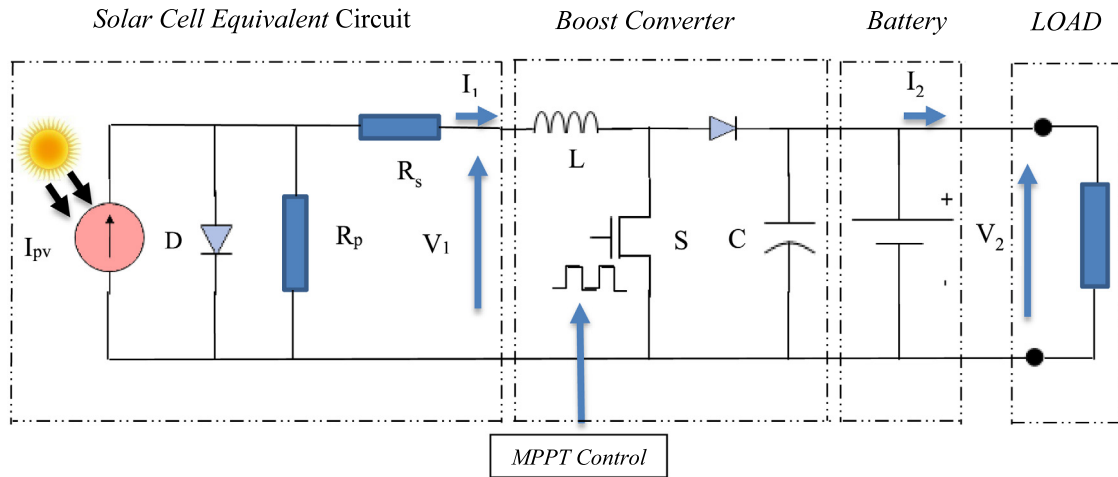


Fig. 1. Photovoltaic system.

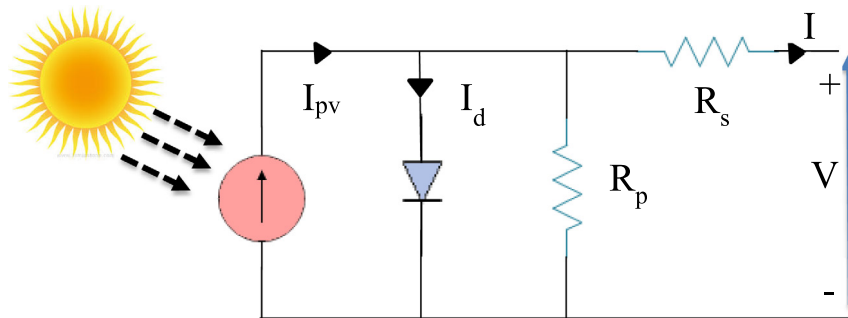


Fig. 2. Solar panel equivalence circuit.

current method. Intelligent systems such as neural networks (NN) and fuzzy logic controllers (FLC) have been used successfully in tracking the maximum power point of PV to decrease computation power requirement, while increasing the speed and efficiency of the tracking. They are robust and relatively simple to design. This is because that this paper presents a Fuzzy Logic Controller (FLC) for tracking maximum power point. FL controller in the mentioned studies uses voltage and PV current to calculate output current variations  $I(k) - I(k - 1)$  and output voltage variations  $V(k) - V(k - 1)$ . Studies (Bahgat et al., 2005, 2004) estimated MPPT by NN method. This study proposed a fuzzy logic-based hybrid method for maximum power point tracking. In this method, the maximum power point is approximate using offline short circuit current and then accurate value of maximum power is calculated based on FL method.

This study includes three sections. Section 2, introduces the PV system. Section 3, presents the proposed method for maximum power point tracking and Section 4, and discusses the simulation and its results.

## 2. Photovoltaic system

A photovoltaic system includes solar panel, battery, DC-DC voltage converter and controller. Fig. 1 illustrates the photovoltaic system used in this study.

As indicated in Fig. 1, the system comprises of various parts, each of which will be explained separately.

### 2.1. Solar panel

The physical structures of a solar panel and a diode are similar in that p-n junction is exposed to light. Observed energy results

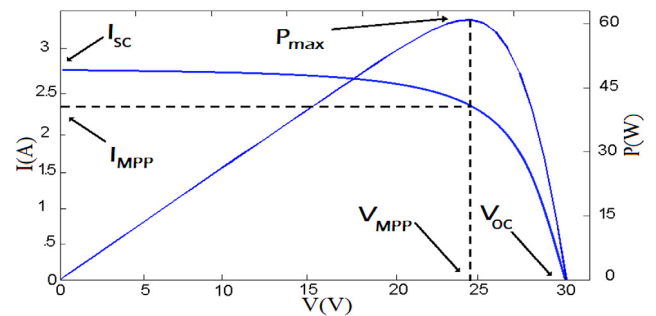


Fig. 3. Voltage-current and voltage-power characteristics of a 60 W solar panel.

from light intensity in this part cause carrier production and transition and collect them in the output terminal. Eqs. (1) and (2), which define semi-conductor theory, describe the features of an ideal cell I-V (Villalva et al., 2009).

$$I = I_{pv,cell} - I_d \tag{1}$$

$$I_d = I_{o,cell} \left[ \exp\left(\frac{qV}{aKT}\right) - 1 \right] \tag{2}$$

where  $I_{pv, cell}$  is the current produced from light radiation,  $I_d$  is diode current modeled by the equation for a Shockley diode,  $I_{a,cell}$  is saturated reverse current or leakage current,  $q$  is the charge of an electron,  $k$  is Boltzmann constant,  $T$  is temperature of p-n junction and “ $a$ ” is diode ideality factor. Fig. 2 indicates the equivalent circuit of a solar panel. A photovoltaic panel consists of several photovoltaic cells, each including internal series, parallel junction or series-parallel. Considering the parameters of Fig. 2

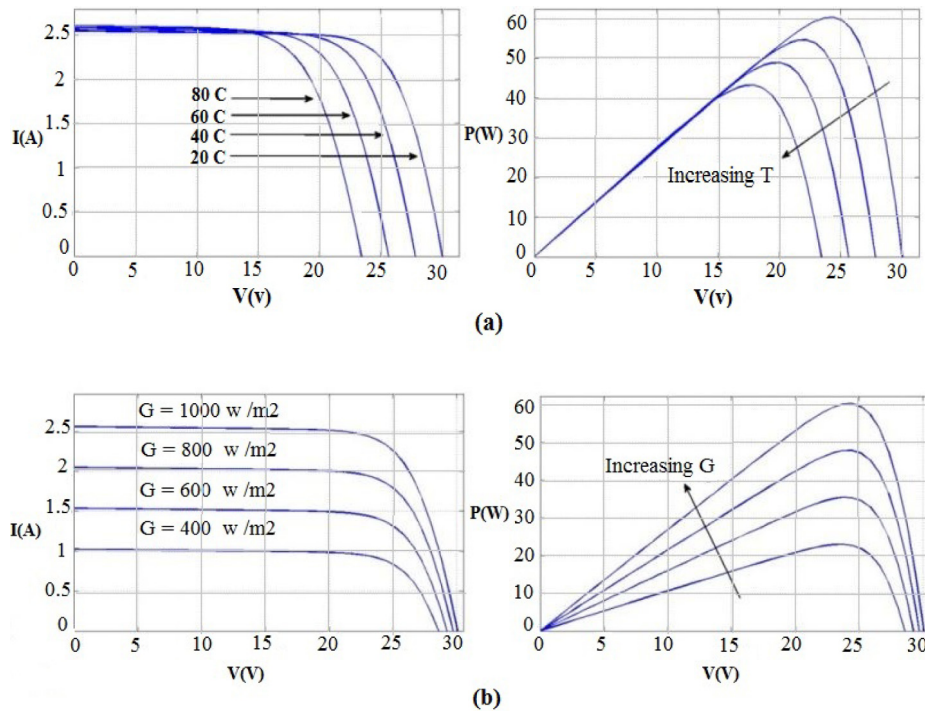


Fig. 4. The effect of ambient temperature and irradiation variations on P-V and I-V curves.

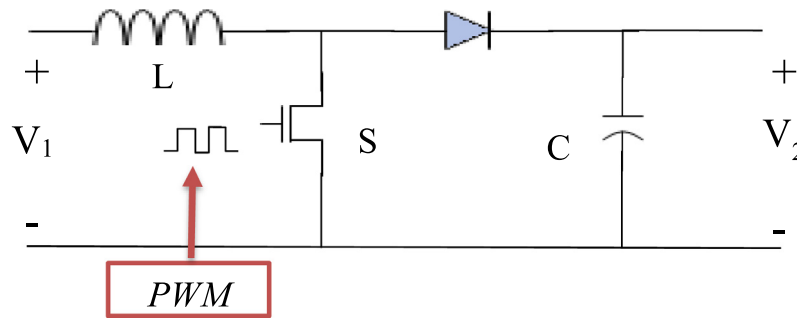


Fig. 5. Boost converter.

in Eq. (1), the properties of the solar panel are obtained and illustrated in Fig. 3 (Moradi et al., 2013).

$$I = I_{pv} - I_o \left[ \exp\left(\frac{V + R_s I}{aV_t}\right) - 1 \right] - \frac{V + R_s I}{R_p} \quad (3)$$

where  $I_{pv}$  is photovoltaic current,  $I_o$  is saturated reverse current,  $V_t = \frac{N_s k T}{q}$  is thermal voltage,  $N_s$  is the number of series cells and  $R_s$  and  $R_p$  are the series and parallel equivalent resistance related to the solar panel.  $I_{pv}$  and  $I_o$  are given by the relation below:

$$I_{pv} = (I_{pv,n} + K_I \Delta T) \frac{G}{G_n} \quad (4)$$

$$I_o = I_{o,n} \left(\frac{T}{T_n}\right)^3 \exp\left[\frac{qE_g}{aK} \left(\frac{1}{T_n} - \frac{1}{T}\right)\right] \quad (5)$$

where  $I_{pv,n}$  is photovoltaic current under standard conditions ( $G_n = 1000 \text{ W/m}^2$  and  $T_n = 25 \text{ }^\circ\text{C}$ ),  $K_I$  is the temperature coefficient of the short circuit current,  $\Delta T = T - T_n$  is deviation from standard temperature,  $G$  is light intensity and  $E_g$  is the band gap energy of semiconductor in units electron-volts.  $I_{o,n}$  is saturated reverse current and is given by the following equation.

$$I_{o,n} = \frac{I_{sc,n}}{\exp\left(\frac{V_{oc,n}}{aV_t}\right)} \quad (6)$$

where  $I_{sc,n}$  is the circuit current and  $V_{oc,n}$  is the open circuit voltage under standard conditions. “a” is a constant between 1 and 1.5, which depends on the other parameters of the model (Carrero et al., 2007). Proper selection of “a” enhances the accuracy of the model. Instead of Eq. (5), the following relation, in which  $K_V$  is the temperature coefficient of the open circuit voltage, increases the accuracy of the model (Villalva et al., 2009).

$$I_o = \frac{I_{sc,n} + K_I \Delta T}{\exp(V_{oc,n} + K_V \Delta T) / aV_t - 1} \quad (7)$$

The Open Circuit Voltage and Short Circuit Current are significant elements related to the IV properties of the solar panel. These elements change with changes in atmospheric conditions. The Short Circuit Current and Open Circuit Voltage can be calculated under different atmospheric conditions using Eqs. (8) and (9) which are derived from the modeled equations.

$$I_{sc} = (I_{sc,n} + K_I \Delta T) \frac{G}{G_n} \quad (8)$$

$$V_{oc} = V_{oc,n} + K_V \Delta T \quad (9)$$

Fig. 4 shows I-V and P-V properties for various light intensity values and temperatures. As indicates in the figure, the Open Circuit Current has an inverse association with temperature (Fig. 4(a)),

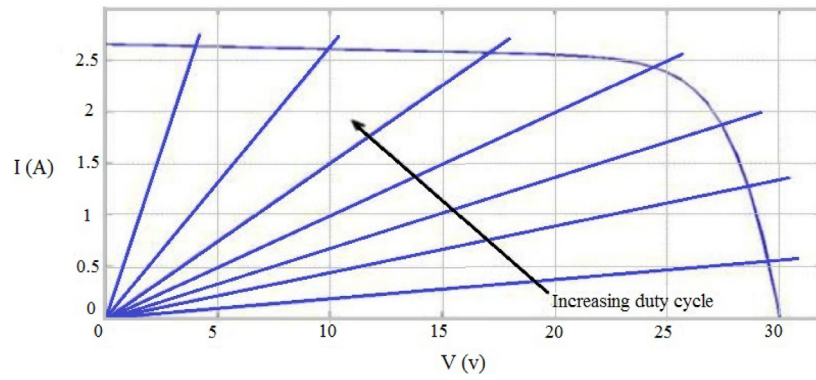


Fig. 6. Load impedance variation from cell view by boost inverter.

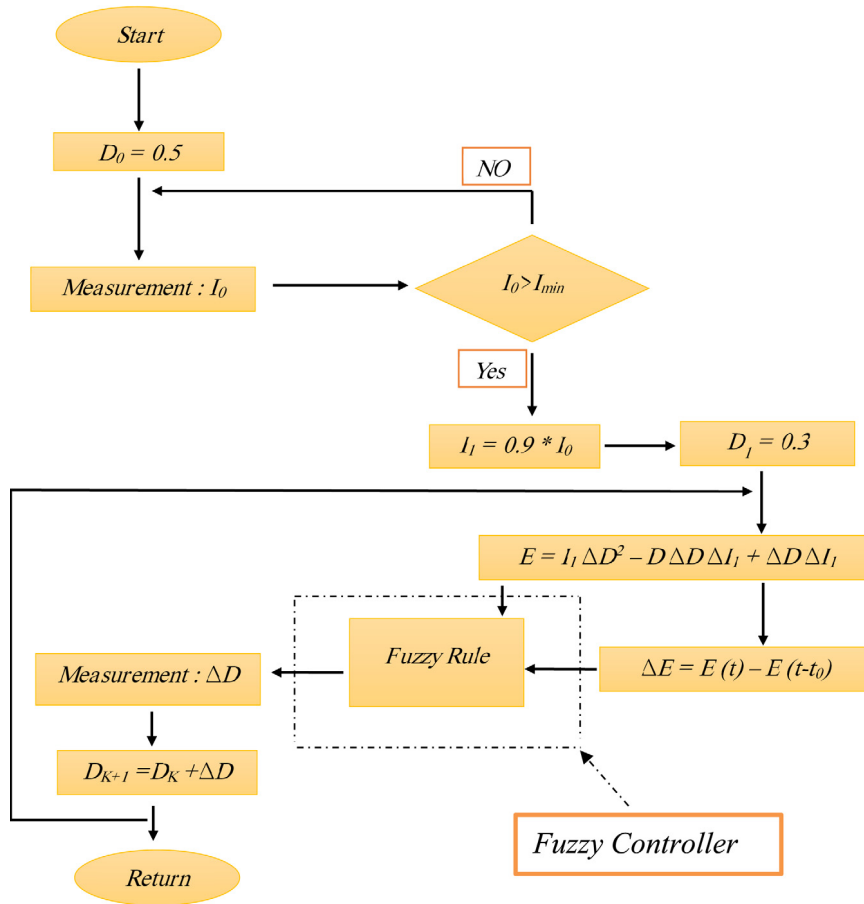


Fig. 7. Proposed method algorithm.

i.e. as temperature increases, Open Circuit Voltage and maximum power reduce, but there is a direct relationship between Short Circuit Current and light intensity. (Fig. 4(b)) Short Circuit Current and maximum power increase with a rise in light intensity.

2.2. DC–DC voltage converter

The choice of DC–DC voltage converter is dependent on the amount of voltage variations. Existence of converter is essential for matching the panel curve, battery and output load at maximum power point (Tasi-Fu and Yu-Kai, 1998). Moreover, the converter is responsible for impeding and control matching. DC–DC voltage converters are divided into three groups, including boost converters, buck converters and buck-boost converters. In

this study, boost DC–DC voltage converter was utilized to match the load and solar panel, indicated in Fig. 5.

According to boost DC–DC voltage converter equation, where D is duty cycle, we have:

$$\frac{V_2}{V_1} = \frac{1}{1 - D} \tag{10}$$

$$V_1 = V_2 * (1 - D) \tag{11}$$

$$\text{IF } V_1 = V_{MPP} \text{ Then } D = D_{MPP} \tag{12}$$

The above equations show that the solar panel power point can be changed by D value variation. Also according to  $V_{MPP}$  uniqueness, there is only one unique value for  $D_{MPP}$ , which puts the solar panel power point in MPP.

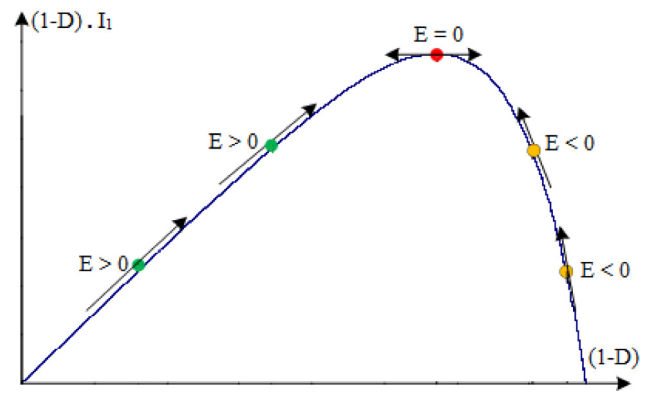
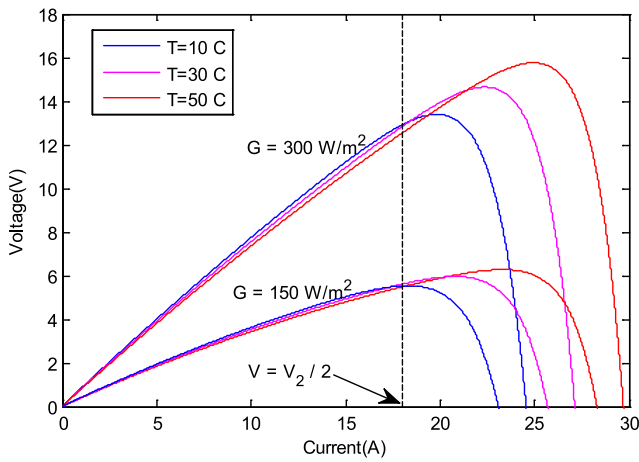


Fig. 9. Power and error curve.

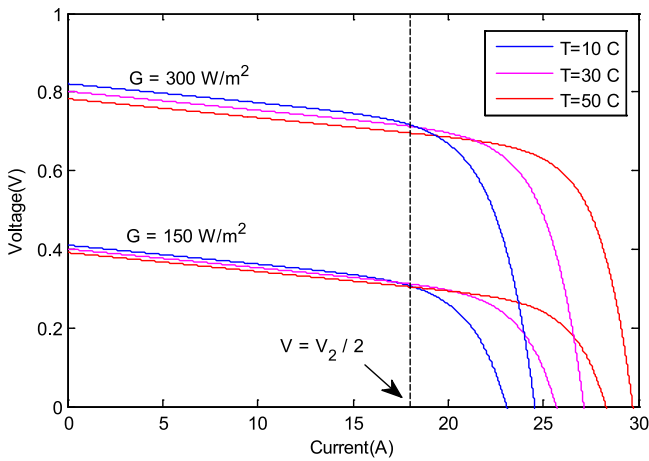


Fig. 8. V-P and V-I characteristics of solar cell in low light intensity and  $D = 0.5$ .

### 2.3. Load and battery

In order for the photovoltaic system to perform as a real source, i.e. to have a constant level of voltage in various loads, battery is used. Battery is also required to store energy and carry out sectional compensation (Moradi and Reisi, 2011). The voltage of battery is usually considered to be an exhausted battery or an empty battery. When internal resistance increases, the output

voltage is not constant. In this case, a DC source and a resistance are used to model the battery.

#### 2.3.1. Equivalent circuit of load and battery

Equivalent Thevenin circuit can be used to model the battery and load, which consists of voltage source  $V_{th}$  and resistance  $R_{th}$ . The elements of this equivalent circuit changes with battery charging and discharging. In other words, charging and discharging the battery results in  $V_{th}$  variations and  $R_{th}$  alters with changes in load and battery exhaustion. In order to obtain  $R_{th}$  and  $V_{th}$ , voltage and output current must be obtained in two conditions in which irradiation and temperature variation is intense and put it in Eq. (6).

Therefore we have two equations of two unknowns, where  $R_{th}$  and  $V_{th}$  can be obtained easily.

$$V_o = R_{th} * I_o + E_{th} \tag{13}$$

In the solar panel voltage current, merely one power point exists, in which voltage–current curve characteristics have to cross this point in order to obtain it. An inverter can change the observed load so as to achieve maximum power point. Fig. 6 illustrates this issue.

### 2.4. MPPT algorithm

Generally, various types of MPPT algorithms can be classified into three categories depending on the model which is offline, independent of the model which is online and the model which is hybrid (Moradi and Reisi, 2011). Various online and offline

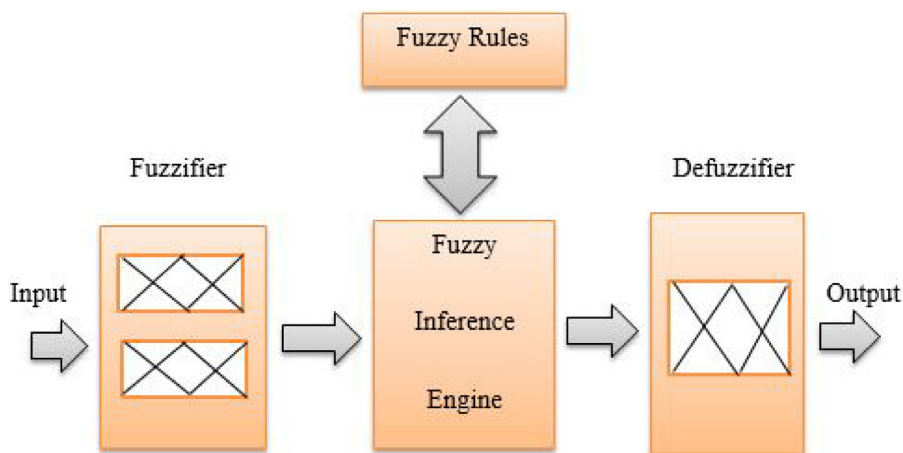
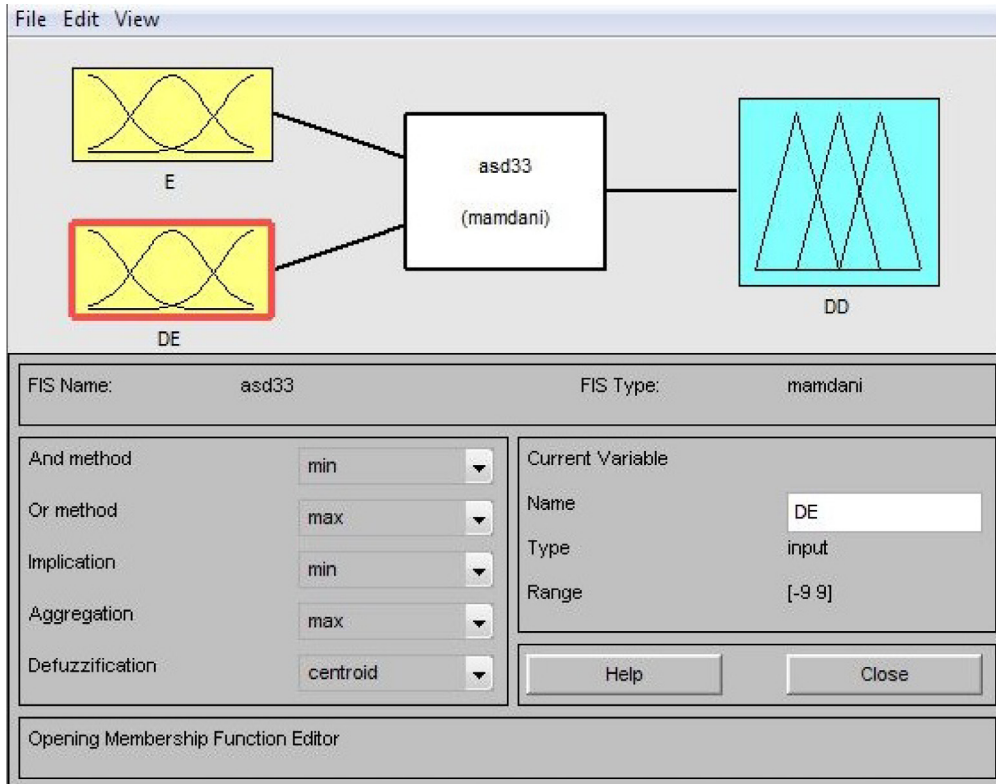
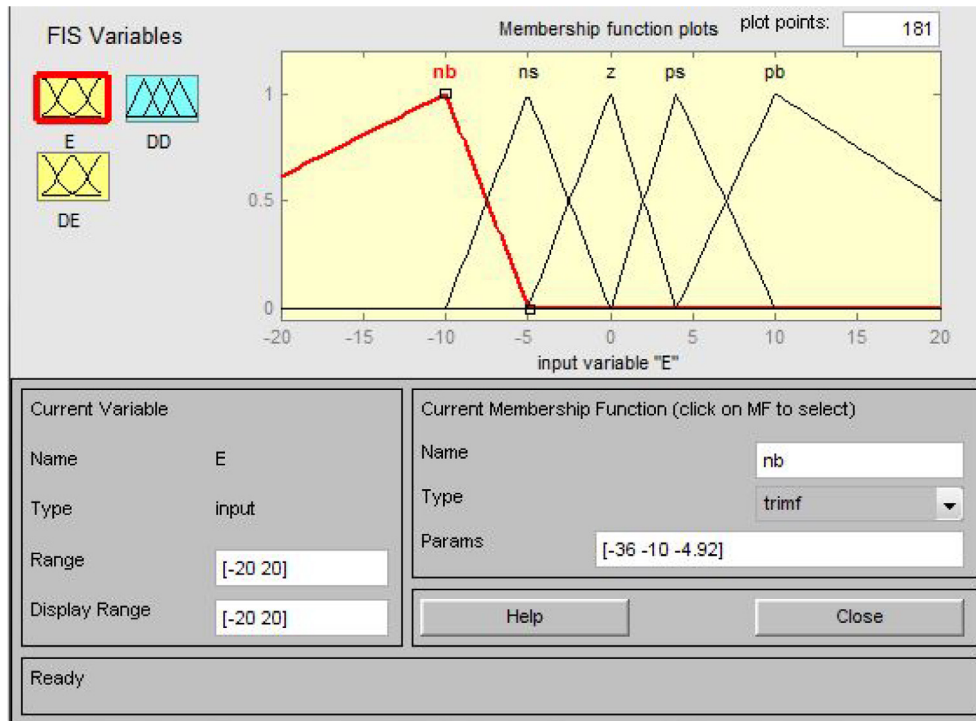


Fig. 10. General scheme of fuzzy controller.

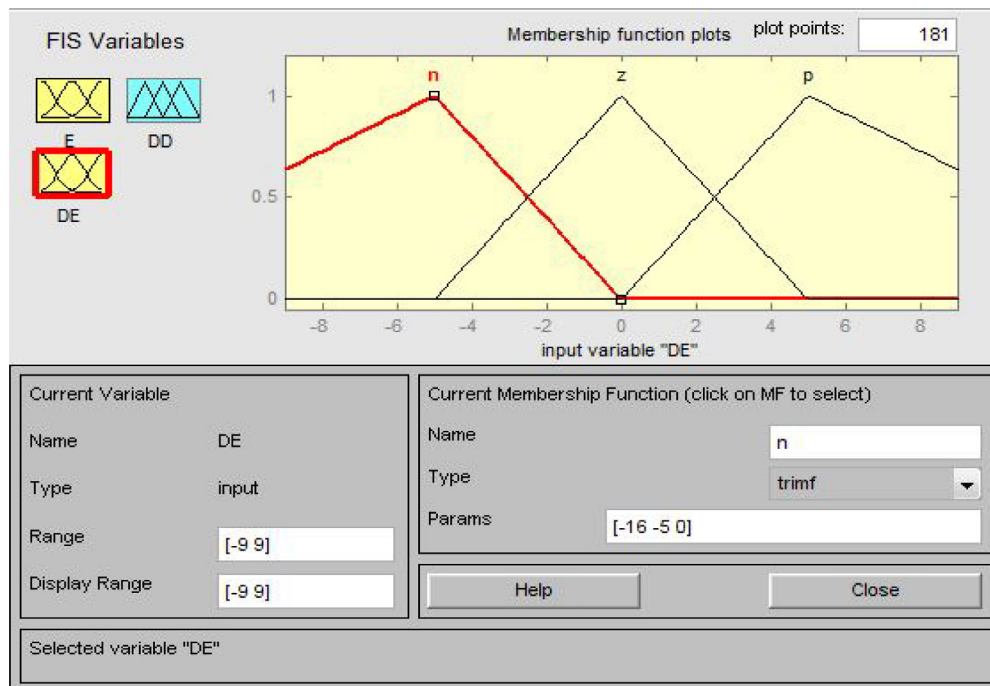


a)

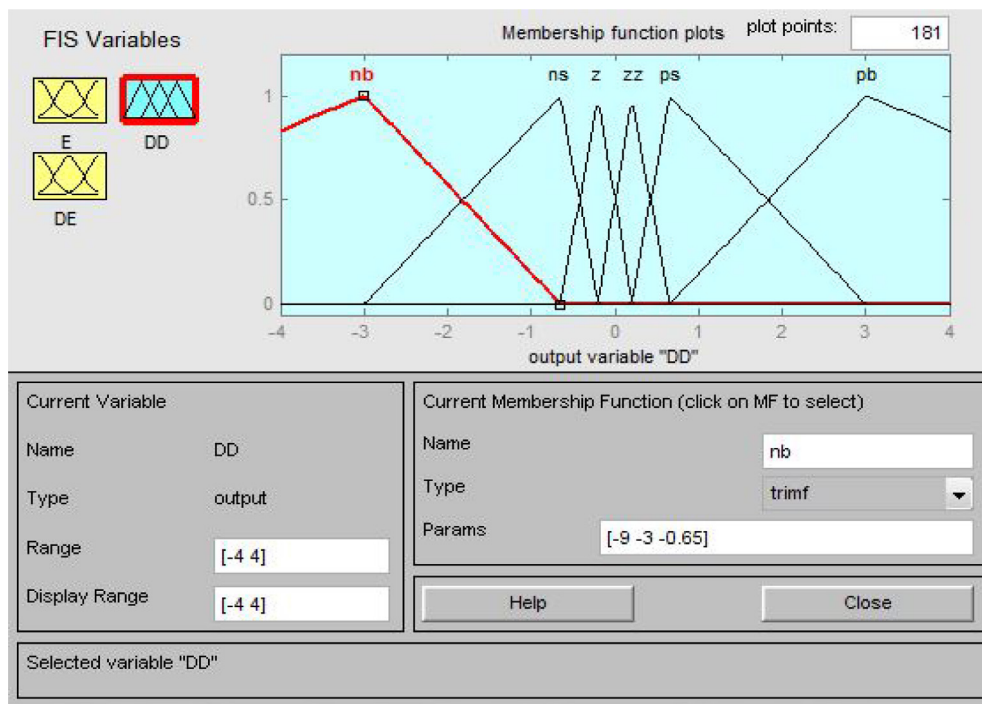


b)

Fig. 11. (a) Proposed fuzzy logic controller and membership functions: (b) Error (E) (c) Error variations ( $\Delta E$ ) (d) Duty cycle (D) variations.



c)



d)

Fig. 11. (continued).

methods have been investigated in [Esrām and Chapman \(2007\)](#), some of which will be discussed below. Using the primary data and solar panel input variables such as light intensity, temperature, Open Circuit Voltage and Short Circuit Current, the offline methods control the signal, and this signal is utilized to control the output power of the panel during the system exploitation. Open Circuit Voltage (OCV), Short Circuit Current (SCC)

and methods based on Artificial Intelligence (AI) like Neural Network (NN) and Fuzzy Logic (FL) are Offline methods ([Schoeman and Van Wyk, 1982](#); [Enslin et al., 1997](#); [Noguchi et al., 2002](#); [Hiyama et al., 1995b,a](#)). In online methods, temporal values of solar panel variables are usually used to produce control signal. Contrary to offline methods, control signal in these methods is not a constant value and oscillates around optimum value in



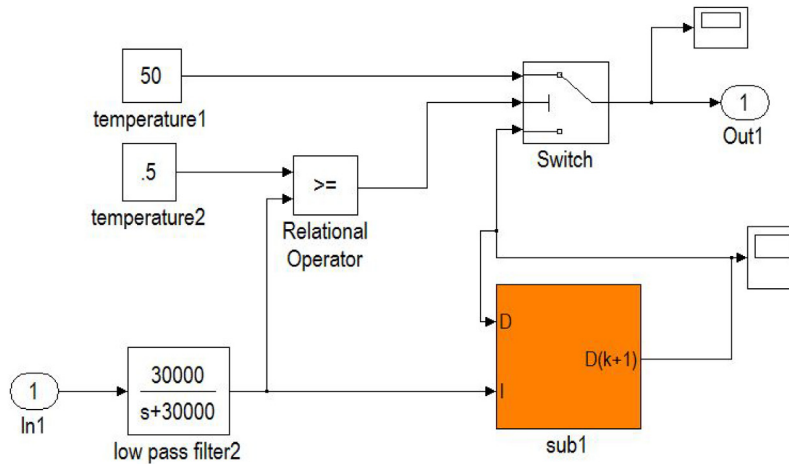
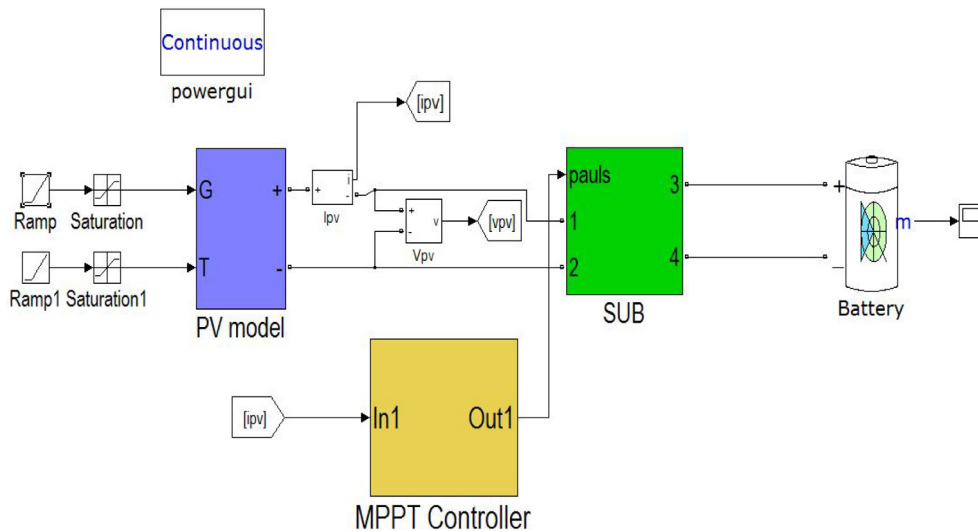


Fig. 12. Simulated photovoltaic system in MATLAB work space.

steady state. Perturbation and Observation method [P&O], Ripple Correlation Control method (RCC) (Chen et al., 2004) and Incremental Impedance (Inc Cond) are online maximum power point tracking methods which produce proper control signal by solar panel output voltage and current (Moradi et al., 2013; Hua et al., 1998; Chen et al., 2004; Huynh and Cho, 1996; Hussein et al., 1995; Eram et al., 2006; Zhi-dan et al., 2008; Hua and Lin, 2003; Yu et al., 2004; Tafticht et al., 2008; Ben Salah et al., 2008). In Moradi and Reisi (2011), a hybrid method (online–offline) was presented for maximum power point tracking, where maximum power point was approximated based on Open Circuit Voltage (OCV) method (offline), then accurate rate of maximum power was calculated according to Perturbation and Observation (P&O) method. This study presented a new combined (online–offline) method for maximum power point tracking. In this method maximum power point is approximated by Short Circuit Current (SCC) (offline) and then accurate value of power point is calculated using Fuzzy Logic method.

### 3. Proposed method

As it was mentioned, a PV system consists of solar panel, control section, battery and voltage converter, as shown in Fig. 1. In this system, the solar panel is attached to a constant voltage DC bus  $V_2$  by an incremented voltage converter. In this case, the

battery with  $V_2$  voltage plays the role of DC bus. The produced power is as follows:

$$P = V_1 * I_1 = V_2 * I_2 \quad (14)$$

Calculating  $V_1$  voltage in incremental voltage converter based on voltage  $V_2$  which is a constant value, and duty cycle, we have:

$$\frac{V_2}{V_1} = \frac{1}{1-D} \rightarrow V_1 = (1-D)V_2 \quad (15)$$

$$P = (1-D)V_2 * I_1 \quad (16)$$

In maximum power point tracking we are perusing  $V_1$  and  $I_1$  to have the highest rate. According to Eq. (20) and considering the fact that  $V_2$  is constant, the highest power is obtained when “ $(1-D).I_1$ ” phrase value has the highest rate, it means we have:

$$\text{Max} : \{P = V_1.I_1\} = \text{Max} : \{(1-D)V_2.I_1\} \quad (17)$$

The proposed algorithm, which is a hybrid method, consists of “approximation” and “accurate adjustment”. Each ring completes the other performance as a series to track the maximum power point, as indicated in Fig. 7.

Approximate maximum power point is estimated in approximation part. In the presented method, the maximum power point value is estimated according to the Short Circuit Current. Knowing Short Circuit Current value is accompanied by light intensity variations, approximate power point value is calculated. This is

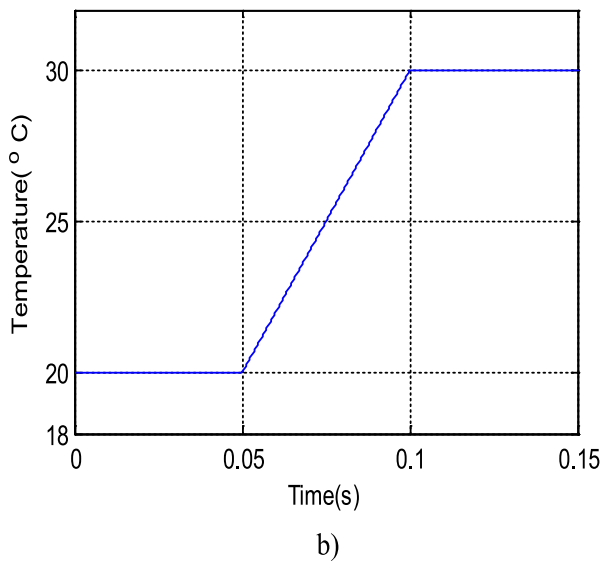
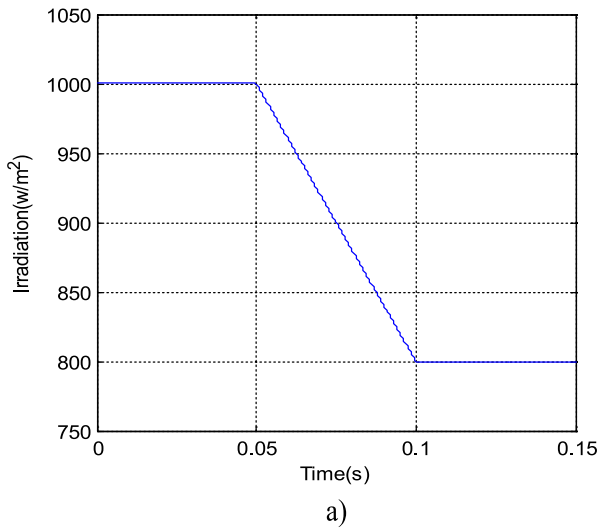


Fig. 13. (a) Radiation variation (b) temperature variations.

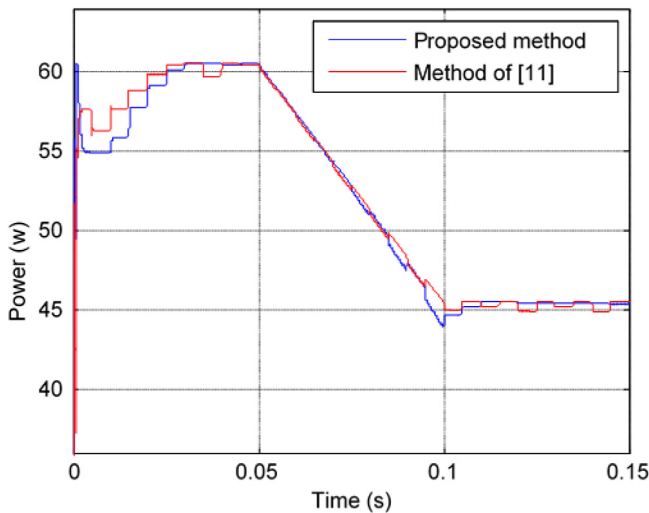


Fig. 14. Output power.

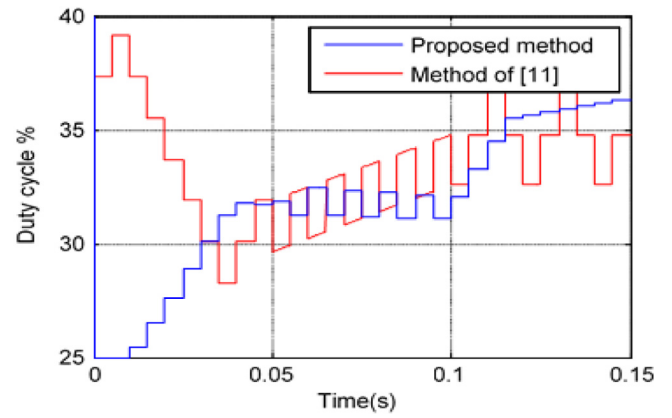


Fig. 15. Duty cycle.

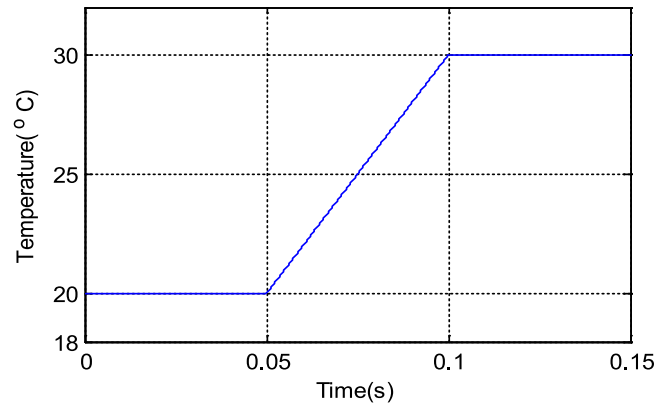


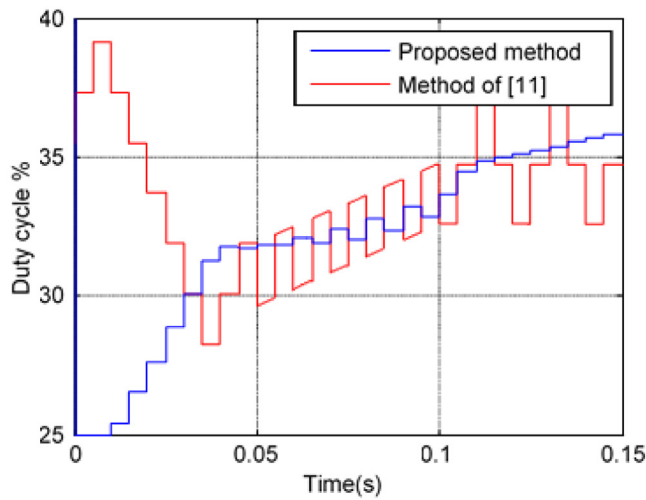
Fig. 16. Temperature variations.

done based on the semi-linear relation between the Short Circuit Current and maximum current power which is shown in Eq. (15). Measuring Short Circuit Current requires solar panel separation from load and connecting it to another short circuit. This method, which is done in Short Circuit Current, decreases the system efficiency and increases the costs of methods. In the proposed method, duty cycle ( $D$ ) value is considered to be 0.5 in order to measure short circuit current value. In this regard, considering the investigations done on the solar panel voltage–current curve for various atmospheric conditions, the measured current is equal to short circuit current with a proper approximation, Fig. 8. When  $D = 0.5$ , the solar panel voltage value sets in half of DC bus voltage value.

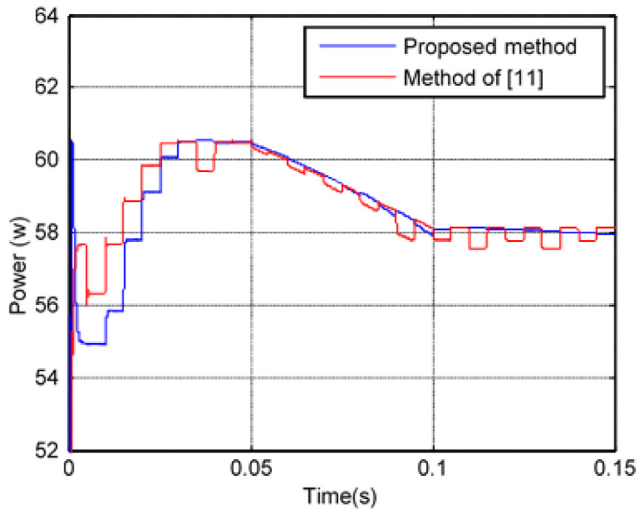
In a state when current value is lower than a certain value, ( $I_{min}$ ) algorithm does not start, and current measurement will restart after a short pause. If the current value is bigger than  $I_{min}$ , the algorithm enters its first ring. In this case, the approximated current is supported to be equal to circuit current, and approximate value of maximum power point is estimated. In this algorithm, the aim is extracting the maximum power by maximizing “ $(1-D) \cdot I_1$ ” value. In this phrase, whose curve is similar to V-P curve, there is one maximum point. Through derivation from power function to determine maximum value, we have:

$$\frac{dP}{d(1-D)} = 0 \tag{18}$$

$$\rightarrow V_2 \left( I_1 - (1-D) \frac{dI_1}{d(1-D)} \right) = 0 \tag{19}$$



a)



b)

Fig. 17. (a) Duty cycle and (b) output power.

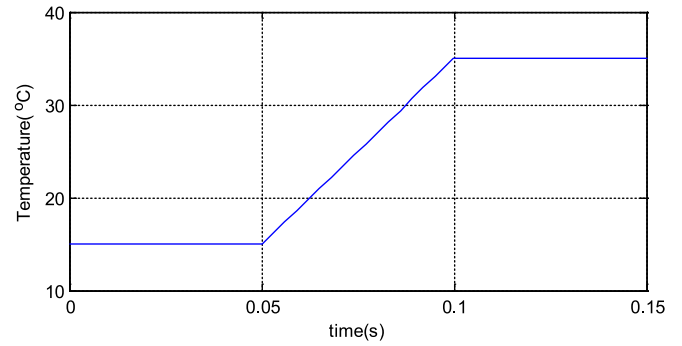
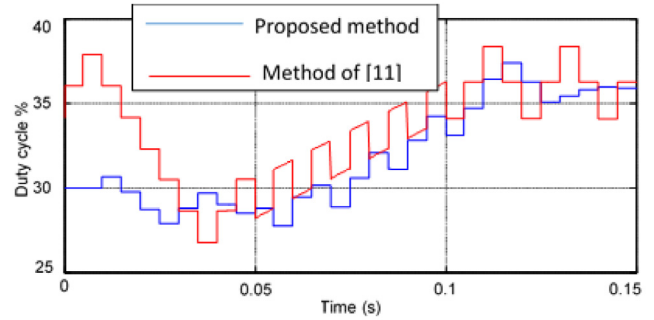
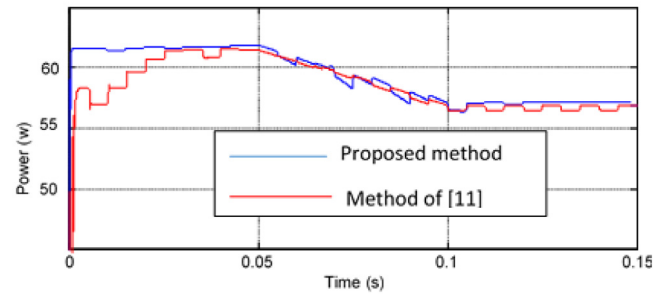


Fig. 18. Temperature variations.



a)



b)

Fig. 19. (a) Duty cycle and (b) output power.

Simplifying the above phrase and considering the variations of parameters, we have:

$$I_1 - \frac{D\Delta I_1}{\Delta D} + \frac{\Delta I_1}{\Delta D} = 0 \tag{20}$$

This phrase is at maximum power point, and it is negative or positive for the other points of the curve. Positive value results from the left side of the maximum power point and negative value results from the right side of the maximum power point value. Phrase value determines the error rate in this algorithm, Fig. 9. This phrase determines the controller input error rate, which is designed based on fuzzy logic.

To modify these conditions, we multiply Eq. (20) by  $\Delta D^2$  value, and then we have:

$$E = I_1 \cdot \Delta D^2 - D\Delta I_1 \Delta D + \Delta I_1 \Delta D \tag{21}$$

In this case, error rate is a function of duty cycle variations, and as these variations are determined by the controller, the controller

can analyze them. Knowing the error rate is necessary and sufficient for controller designing. Calculating  $E$  and its variation  $\Delta E$ , duty cycle value variation is calculated.

### 3.1. Proposed fuzzy algorithm method

Fuzzy controller is a potent control methods, which is based on multi-variations by multi-laws (Tafticht et al., 2008). Using expert knowledge and data bases, Fuzzy Logic gives faster results than other methods such as GA and NN. Hence, Fuzzy control method is selected as a managerial tool for the existing systems. The general schematic of Fuzzy controller is illustrated in Fig. 10.

Here,  $E$  and  $\Delta E$  are Fuzzy controller variable inputs and  $\Delta D$  is output variable. The mentioned variables go to the deduction machine after fuzzification and after applying the rules, they enter the defuzzification part. Finally, the controller produces a real value, which is  $\Delta D$ . Fig. 11 illustrates the proposed Fuzzy Logic Controller.

**Table 1**  
Fuzzy rules set.

$E$	$\Delta E$		
	$n$	$z$	$p$
$nb$	$Z$	$Z$	$Z$
$ns$	$NS$	$NS$	$NS$
$z$	$ZZ$	$ZZ$	$ZZ$
$ps$	$PS$	$PS$	$PS$
$pb$	$Z$	$Z$	$Z$

**Table 2**  
Solar panel characteristics.

Variables	Values
$I_{mp}$	2.5 (A)
$V_{mp}$	23.1 (V)
$P_{max,m}$	60 (W)
$I_{sc}$	2.66 (A)
$V_{oc}$	30 (V)
$K_v$	-0.356 (V/K)
$K_I$	0.024 (A/K)

**Table 3**  
Circuit parameters.

Solar cell	$R_s = 0.221 \Omega$ $R_p = 415 \Omega$
Boost converter	$L = 0.82 \text{ mH}$ $C = 2 \text{ mF}$
Battery	Nom Voltage = 36 V Rated Capacity = 2 Ah Initial State-of-charge = 80%

Fuzzy rules set are designed so that the value of  $E$  approaches zero. These rules set are indicated in Table 1.

Voltage converter control signal ( $D_{MPP}$ ) can be controlled by the proposed algorithm.

**4. Simulation results**

To investigate the method proposed in this study, the photo-voltaic system is shown in Fig. 3, which includes a 60 W solar panel Table 2, a boost voltage converter and a 36 V lead-acid battery simulated in MATLAB/SIMULINK work space, as indicated in Fig. 12.

The circuit parameters are included in Table 3:

Then, the proposed method is applied as a controller, and the findings are compared with the results of the method (Moradi and Reisi, 2011), follows:

- variable radiation and temperature
- constant radiation and variable temperature
- constant temperature and variable radiation
- load variations in constant radiation and temperature
- efficiency
- number of sensors required
- variable radiation and temperature
- variable radiation and temperature

In this experiment, irradiation and temperature increased with the slope of  $-4000 \text{ W/m}^2$  and  $10 \text{ e/s}$ , respectively, as illustrated in Fig. 13.

Applying this radiation and temperature to the system, the output power and the duty cycle for these conditions are indicated in Figs. 14 and 15, respectively.

- constant radiation and variable temperature

In this experiment, radiation is constant and equal to  $1000 \text{ W/m}^2$ , but temperature changes over time, Fig. 16.

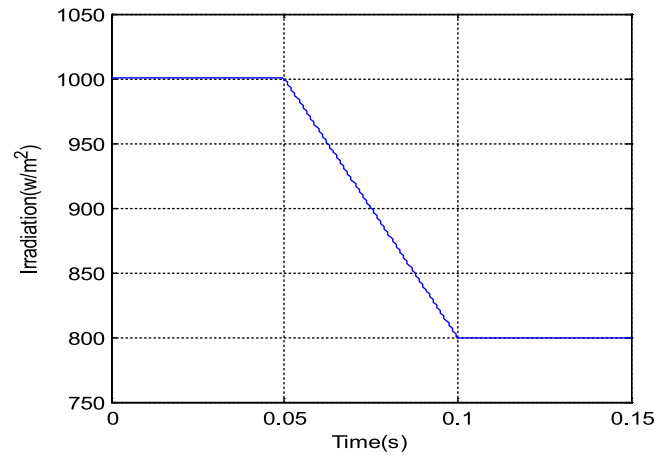
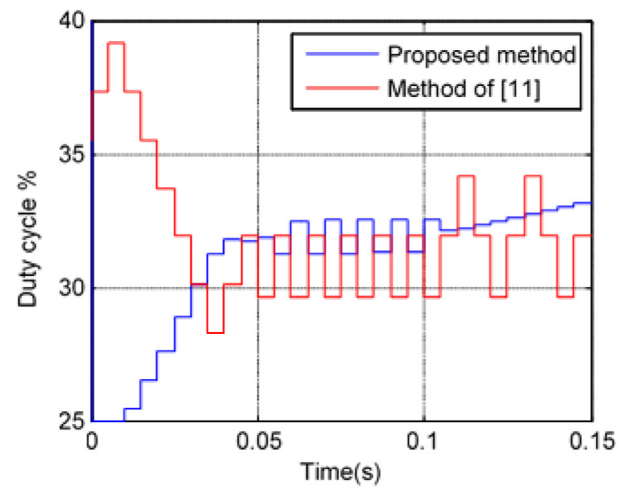
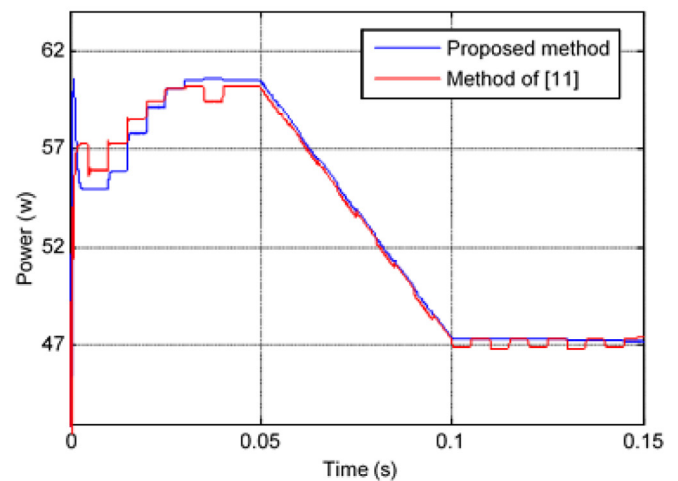


Fig. 20. Radiation variations.



a)



b)

Fig. 21. (a) Duty cycle and (b) output power.

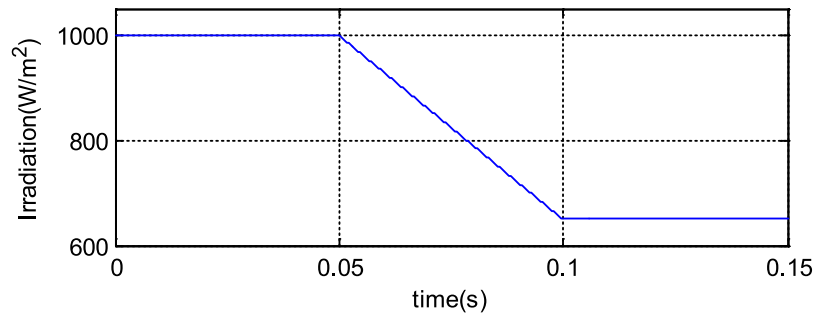


Fig. 22. Radiation variations.

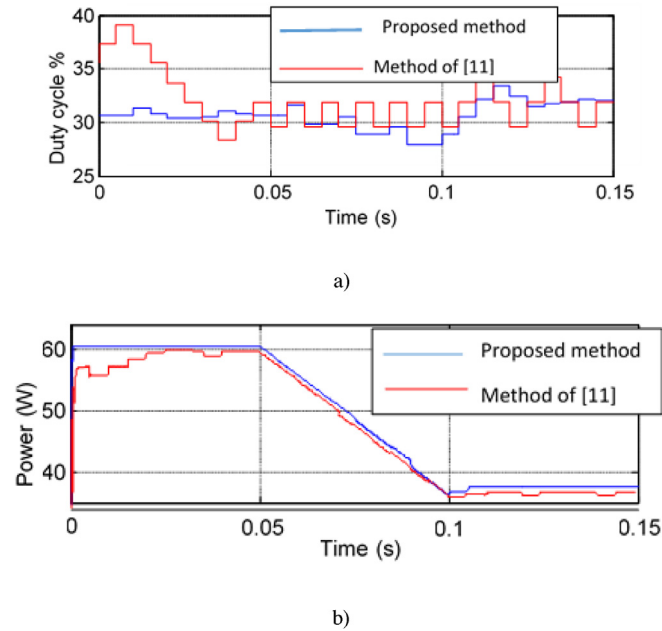


Fig. 23. (a) Duty cycle and (b) output power.

Applying this radiation and temperature to the system, the duty cycle and the output power for these conditions are illustrated in Fig. 17(a) and (b), respectively.

In this experiment, radiation is constant and equals to 1000 W/m<sup>2</sup>, but temperature changes over time, Fig. 18.

Applying this radiation and temperature to the system, the duty cycle and the output power for these conditions are illustrated in Fig. 19(a) and (b), respectively.

- Constant temperature and variable radiation.

In this simulation, the performances of available methods at 20 °C and variable radiation, as shown in Fig. 20, are compared.

Applying this radiation and temperature to the system, the duty cycle and the output power for these conditions are indicated in Fig. 21(a) and (b), respectively.

In this simulation, the performances of available methods at 25 °C and variable radiation, as shown in Fig. 22, are compared.

Applying this radiation and temperature to the system, the duty cycle and the output power for these conditions are indicated in Fig. 23(a) and (b), respectively.

In this section in order to highlight the effectiveness of the proposed method, the comparison between the proposed method and the other fast and most recent methods has been made. For doing this, radiation is 1000 W/m<sup>2</sup> and temperature changes over time is in Fig. 24.

Applying this radiation and temperature to the system, the output power for these conditions is indicated in Fig. 25.

- Load variations

In this test, at t = 0.05 s by a switch, a 20 Ω resistance is put to the two ends of the battery. Here, radiation is 1000 W/m<sup>2</sup> and temperature is 25 °C. Fig. 26 illustrates voltage and current variations at the two ends at the time of resistance entrance. Therefore, the output power is shown in Fig. 27.

- Efficiency

One of the most important parameters which is always in focus and is of high importance is method efficiency. Relation 22 is utilized to compare the efficiencies of different of maximum power point tracking methods.

$$\eta_T = \frac{1}{n} \sum_{i=0}^n \frac{P_i}{P_{max,i}} = \frac{1}{n} \sum_{i=0}^n \left( 1 - \frac{P_L}{P_{max,i}} \right) \quad (22)$$

where  $P_i$  is the power of solar panel,  $P_{max,i}$  is the maximum power of solar panel,  $P_L = (P_{max,i} - P_i)$  is the loss of power and  $n$  is the number of examples. In this relation, maximum power ( $P_{max}$ ) is commensurate to light intensity. Steady state

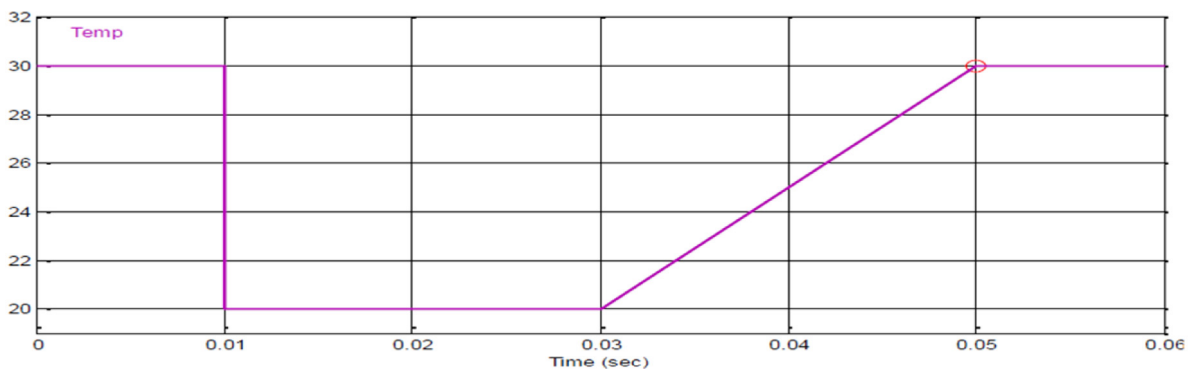


Fig. 24. Temperature variation.

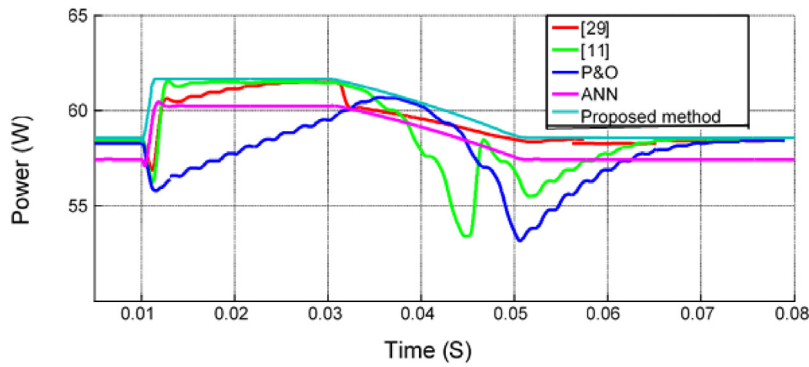


Fig. 25. Output power.

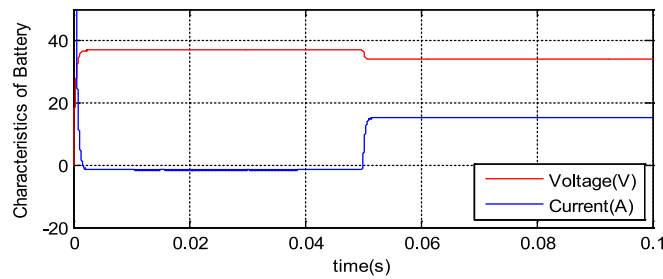


Fig. 26. Load variations.

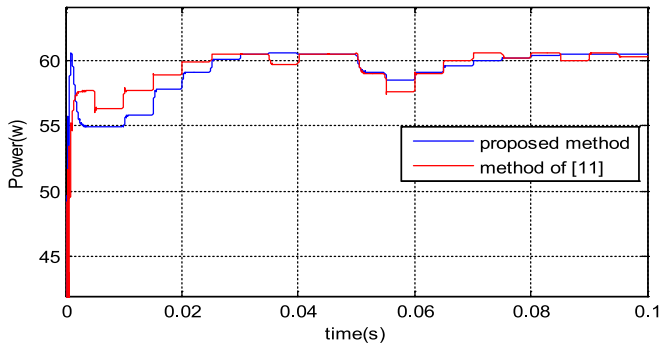


Fig. 27. Output power in load variations.

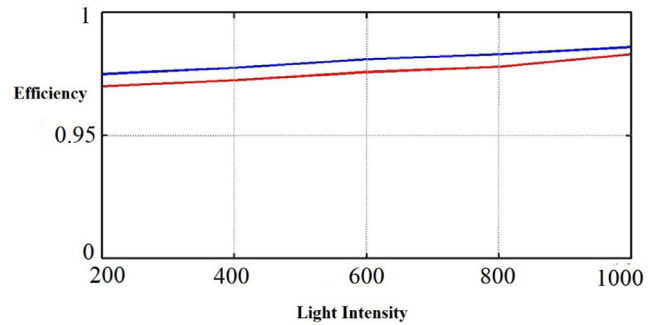


Fig. 28. Efficiency curve for the mentioned methods. (For interpretation of the references to color in this figure legend, the reader is referred to the web version of this article.)

Table 4

Detail comparison of efficiency.

Irradiance (W/m <sup>2</sup> )	200	400	600	800	1000
Proposed method efficiency %	97.5	97.75	98.1	98.3	98.6
Method of Moradi and Reisi (2011) efficiency %	97	97.25	97.58	97.8	98.26

loss ( $P_1$ ) is commensurate to the disturbance amplitude and as disturbance amplitude increases, the loss increases and efficiency declines. In the classical P&O method, the disturbance amplitude is constant and result in power variations in the steady state, which consequently decreases the efficiency.

Fig. 28 and Table 4 illustrate the efficiency curve (blue curve) of proposed method and hybrid method (Moradi and Reisi, 2011) (red curve) and detail comparison of both mentioned method, respectively. Oscillation is very low in the proposed method, so the loss is low and efficiency is high. But in the previous hybrid method in steady state, classic P&O is implemented, and efficiency rate is less than that of the proposed method because of oscillation.

• Number of sensors required

The number of sensors required in an algorithm determines the other characteristics of algorithm. In online methods, minimum parameters of voltage and current are determined. In offline methods, some parameters, including temperature, light intensity, Open Circuit Voltage and etc. are measured. In addition to voltage and current, other parameters like temperature, Open Circuit Voltage, Short Circuit Current and etc. are also measured. Current is the only parameter measured in the proposed method. But duty cycle value is another parameter used in calculating MPP. In addition to making the implementation easy, it reduces the costs of the method from hardware aspects. Table 5 illustrates general comparison between the proposed method and method of Moradi and Reisi (2011).

Conclusion

This study, presented a new Fuzzy Logic-based hybrid method to enhance maximum power point tracking. The presented algorithm consists of two sections, including work point calculation and accurate adjustment. Work point calculation, which is

**Table 5**  
General comparison.

MPPT algorithm	Proposed method (FL)	Method of Moradi and Reisi (2011) (P&O)
Tracking accuracy	Very high	Medium
Sensor numbers	1	2
Digital or analog	Digital	Analog
Convergence speed	Fast	Low

centered on Short Circuit Current, estimates approximate maximum power. Accurate adjustment follows the accurate value of power point based on FL method. Simulation of the proposed method was performed in MATLAB/SIMULINK work space. The findings revealed that the proposed method performed better than method used (Moradi and Reisi, 2011) under different atmospheric conditions. Simplicity, less hardware requirements, low cost of implementation and higher efficiency are merits of the proposed algorithm.

### Declaration of competing interest

The authors declare that they have no known competing financial interests or personal relationships that could have appeared to influence the work reported in this paper.

### References

- Bahgat, A.B.G., Helwa, N.H., Ahamd, G.E., El Shenawy, E.T., 2004. Estimation of the maximum power and normal operating power of a photovoltaic module by neural networks. *Renew. Energy* 29, 443–457.
- Bahgat, A.B.G., Helwa, N.H., Ahamd, G.E., El Shenawy, E.T., 2005. Maximum power tracking controller for PV systems using neural networks. *Renew. Energy* 30, 1257–1268.
- Ben Salah, Ch., Chaaben, M., Ben Ammar, M., 2008. Multi-criteria fuzzy algorithm for energy management of a domestic photovoltaic panel. *Renew. Energy* 33, 993–1001.
- Carrero, C., Amador, J., Arnaltes, S., 2007. A single procedure for helping PV designers to select silicon PV module and evaluate the loss resistances. *Renew. Energy* 32 (15), 2579–2589.
- Chen, Y.M., Liu, Y.C., Wu, F.Y., 2004. Multi-input converter with power factor correction, maximum power point tracking, and ripple-free input currents. *IEEE Trans. Power Electron.* 19, 631–639.
- Enslin, J.H.R., Wolf, M.S., Snyman, D.B., Swiegers, W., 1997. Integrated photovoltaic maximum power point tracking converter. *IEEE Trans. Ind. Electron.* 44, 769–773.
- Esrām, Trishan, Chapman, Patrick L., 2007. Comparison of photovoltaic array maximum power point tracking techniques. *IEEE Trans. Energy Convers.* 22 (2), 439–449.
- Esrām, T., Kimball, J.W., Krein, P.T., Chapman, P.L., Midya, P., 2006. Dynamic maximum power tracking of photovoltaic arrays using ripple correlation control. *IEEE Trans. Power Electron.* 21 (5), 1282–1291.
- Hiyama, T., Kouzuma, S., Imakubo, T., 1995a. Identification of optimal operating point of PV modules using neural network for real-time maximum power tracking control. *IEEE Trans. Energy Convers.* 10 (2), 360–367.
- Hiyama, T., Kouzuma, S., Imakubo, T., Ortmeyer, T.H., 1995b. Evaluation of neural network based real-time maximum power tracking controller for PV system. *IEEE Trans. Energy Convers.* 10 (3), 543–548.
- Hua, C., Lin, J., 2003. An on-line MPPT algorithm for rapidly changing illuminations of solar arrays. *Renew. Energy* 28 (7), 1129–1142.
- Hua, C., Lin, J., Shen, C., 1998. Implementation of a DSP-controlled photovoltaic system with peak power tracking. *IEEE Trans. Ind. Electron.* 45 (1), 99–107.
- Hussein, K.H., Muta, I., Hoshino, T., Osakada, M., 1995. Maximum photovoltaic power tracking: an algorithm for rapidly changing atmospheric conditions. *IEE Proc., Gener. Transm. Distrib.* 142 (1).
- Huynh, P., Cho, B.H., 1996. Design and analysis of a microprocessor-controlled Peak-Power-Tracking system. *IEEE Trans. Aerosp. Electron. Syst.* 32 (1).

- Jain, S., Agarwal, V., 2007. New current control based MPPT technique for single stage grid connected PV systems. *Energy Convers. Manage.* 48, 625–644.
- Kim, S., 2007. Robust maximum power point tracker using sliding mode controller for the three-phase grid-connected photovoltaic system. *Sol. Energy* 81, 405–414.
- Koofigari, Hamid Reza, 2016. Adaptive robust maximum power point tracking control for perturbed Photovoltaic systems with output voltage estimation. *Elsevier ISA Trans.*
- Moradi, Mohammad H., Reisi, Ali Reza, 2011. A hybrid maximum power point tracking method for photovoltaic systems. *Sol. Energy* 85, 2965–2976.
- Moradi, Mohammad H., Reza Tousi, S.M., Nemati, Milad, Saadat Basir, N., Shalavi, N., 2013. A robust hybrid method for maximum power point tracking in photovoltaic systems. *Sol. Energy* 94, 266–276.
- Noguchi, T., Togashi, S., Nakamoto, R., 2002. Short-current pulse-based maximum-power-point tracking method for multiple photovoltaic-and-converter module system. *IEEE Trans. Ind. Electron.* 49 (1), 217–223.
- Radjai, Tawfik, Rahmani, Lazhar, Mekhilef, Saad, Gaubert, Jean Paul, 2014. Implementation of a modified incremental conductance MPPT algorithm with direct control based on a fuzzy duty cycle change estimator using dSPACE. *Sol. Energy* 110, 325–337.
- Radjai, Tawfik, Gaubert, Jean Paul, Rahmani, Lazhar, Mekhilef, Saad, 2015. Experimental verification of P & O MPPT algorithm with direct control based on Fuzzy logic control using CUK converter. *Int. Trans. Electr. Energy Syst. Int. Trans. Electr. Energy Syst.*
- Safari, Azadeh, Mekhilef, Saad, 2011. Simulation and Hardware implementation of incremental conductance MPPT with direct control method using cuk converter. *IEEE Trans. Ind. Electron.* 58, 1154–1161.
- Schoeman, J.J., Van Wyk, J.D., A simplified maximal power controller for terrestrial photovoltaic panel arrays, in *Proc. 13th Annu. IEEE Power Electron. Spec. Conf.* 1982, pp. 361–367.
- Seyedmahmoudian, M., Horan, B., Koksoon, T., Rahmani, R., MuangThanOo, A., Mekhilef, S., Stojcevski, A., 2016. State of the art artificial intelligence-based MPPT techniques for Mitigating partial shading effects on PV systems – A review. *Renew. Sustain. Energy Rev.* 64, 435–455.
- Seyedmahmoudian, Mohammadmehdi, Rahmani, Rasoul, Mekhilef, Saad, Than Oo, Amanullah Maung, Stojcevski, Alex, Soon, Tey Kok, Ghandhari, Alireza Safdari, 2015. Simulation and hardware implementation of new maximum power point tracking technique for partially shaded PV system using hybrid DEPSO method. *IEEE Trans. Sustain. Energy* 6, 850–862.
- Seyedmahmoudian, Mehdi, Soon, Tey Kok, Horan, Ben, Ghandhari, Alireza Safdari, Mekhilef, Saad, Stojcevski, Alex, 2019a. New ARMO-based MPPT technique to minimize tracking time and fluctuation at output of PV systems under Rapidly changing shading conditions. *IEEE Trans. Ind. Inf.*
- Seyedmahmoudian, Mehdi, Soon, Tey Kok, Horan, Ben, Ghandhari, Alireza, Mekhilef, Saad, Stojcevski, Alex, 2019b. New ARMO-based MPPT technique to minimize tracking time and fluctuation at output of PV systems under rapidly changing shading conditions. *IEEE Trans. Ind. Inf.*
- Tafticht, T., Agbossou, K., Doumbia, M.L., Cheriti, A., 2008. An improved maximum power point tracking method for photovoltaic systems. *Renew. Energy* 33 (7), 1508–1516.
- Tasi-Fu, W., Yu-Kai, C., 1998. Modeling PWM DC/DC converters out of basic Converter Units. *IEEE Trans. Power Electron.* 13 (5).
- Tey, Kok Soon, Mekhilef, Saad, 2015. A fast-converging MPPT technique for photovoltaic system under fast varying solar irradiation and load resistance. *IEEE Trans. Ind. Inf.* 11 (1), 176–186.
- Tey, Kok Soon, Mekhilef, Saad, Seyedmahmoudian, Mehdi, Horan, Ben, Than Oo, Amanullah, Stojcevski, Alex, 2018. Improved differential Evolution-based MPPT algorithm using SEPIC for PV systems under partial shading conditions and load variation. *IEEE Trans. Ind. Inf.* 14 (10), 4322–4333.
- Villalva, Marcelo Gradella, Gazoli, Jonas Rafael, Filho, Ernesto Ruppert, 2009. Comprehensive approach to modeling and simulation of photovoltaic arrays. *IEEE Trans. Power Electron.* 24 (5), 1198–1208.
- Yu, C.J., Jung, Y.S., Choi, J.Y., Kim, G.S., 2004. A novel two-mode MPPT control algorithm based on comparative study of existing algorithms. *Sol. Energy* 76 (4), 455–463.
- Zhi-dan, Zhong, Hai-bo, Huo, Xin-jian, Zhu, Guang-yi, Cao, Yuan, Ren, 2008. Adaptive maximum power point tracking control of fuel cell power plants. *Power Sources* 176, 259–269.

### Further reading

- Gounden, N.A., Peter, S.A., Nallandula, H., Krithiga, S., 2009. Fuzzy logic controller with MPPT using line-commutated inverter for three-phase grid-connected photovoltaic system. *Renew. Energy* 34, 909–915.
- Patcharaprakiti, N., Premrudeepreechacharn, S., Sriuthaisiriwong, Y., 2005. Maximum power point tracking using adaptive fuzzy logic control for grid-connected photovoltaic system. *Renew. Energy* 30, 1771–1788.